Epilepsia, **47**(2):277–287, 2006
Blackwell Publishing, Inc.

Decrease of Hippocampal $GABA_B$ Receptor–Mediated Inhibition after Hyperthermia-induced Seizures in Immature Rats

*Min-Lan Tsai and *†‡L. Stan Leung

*Program in Neuroscience, and †Department of Physiology-Pharmacology and ‡Clinical Neurological Sciences, University of Western Ontario, London, Ontario, Canada

Summary: *Purpose:* Whether febrile seizures have detrimental consequences on the brain is still controversial. We hypothesized that neuronal inhibition in the hippocampus is altered after hyperthermia-induced seizures in immature rats.

Methods: Rats were given a single seizure by a heat lamp on postnatal day (PND) 15, or repeated seizures by heated air on PND 13 to 15. Fourteen or 30 days after the seizure(s), laminar field potentials were recorded by 16-channel silicon probes in CA1 and the dentate gyrus (DG), in response to the paired-pulse stimulation of the CA3 and medial perforant path, and analyzed as current source density. γ-Aminobutyric acid $(GABA)_B$-receptor antagonist CGP35348 was injected intracerebroventricularly (icv).

Results: At 14 but not at 30 days after a single or after repeated hyperthermia-induced seizures, paired-pulse facilitation (PPF) of the CA1 population spikes at 100 to 200 ms interpulse intervals (IPIs) was significantly increased in seizure as compared with control rats, irrespective of the types of induced seizures. CGP35348 icv also resulted in PPF at 100 to 200 ms IPIs in CA1 of control rats, but CGP35348 had no effect on PPF in seizure rats. At 30 days after repeated seizures, paired-pulse inhibition in the DG was significantly increased at 30-ms IPI, and PPF was increased at 200-ms IPI. CGP35348 increased paired-pulse inhibition in the DG in repeated-seizure rats but not in control rats.

Conclusions: We conclude that hyperthermia-induced seizures in immature rats induced a decrease of $GABA_B$ receptor–mediated inhibition in CA1 and DG that lasted $\geq$14 to 30 days after hyperthermic seizure(s). **Key Words:** Hyperthermic seizure—CA1—Dentate gyrus—Paired-pulse inhibition—Population spikes—$GABA_B$ receptors—CGP35348.

Febrile seizures (FSs) are the most common type of seizure in children between 3 months and 6 years of age. However, the consequences of FSs on developing or adult brains are not completely understood. It has been proposed that complex FSs are among the risk factors in human temporal lobe epilepsy and temporal lobe sclerosis (1). Furthermore, some evidence from magnetic resonance imaging (MRI) studies has demonstrated focal hippocampal atrophy after prolonged FSs in some children (2,3) and abnormal T_2 signal enhancement in limbic structures in the rat FS model (4).

We have shown an alteration of hippocampal excitability during hyperthermia (5). Hyperthermia (brain temperature $>38.5^{\circ}$C) in urethane-anesthetized rats induced a loss of inhibition in hippocampal CA1 area in immature or adult rats. In contrast, hyperthermia increased inhibition in the dentate gyrus (DG) in the adult but not immature rats under urethane anesthesia (5). Hyperthermia also induced epileptiform activities and spreading depression in brain slices in vitro, with stronger effects on immature as compared with adult brain slices (6,7).

The long-term changes after hyperthermic seizures remain unclear. Prolonged or repeated hyperthermic seizures increased seizure susceptibility in adult rats (8,9) and induced long-term changes in behavior (10). Contrary to other seizure models that show reduced γ-aminobutyric acid (GABA)ergic inhibition (11), a prolonged hyperthermic seizure was reported to increase $GABA_A$ receptor–mediated inhibitory postsynaptic potentials in hippocampal CA1 neurons in vitro (12), and abnormal activation of intrinsic Ih channels at hyperpolarized voltage was proposed to be the cause of increased neuronal excitability (13). Long-term increased excitability in the developing brain was reported in recurrent seizure models in immature rats (14).

We hypothesize that neuronal inhibition in the hippocampus is altered after hyperthermic seizures in immature rats. Neuronal inhibition was assessed by paired-pulse responses in anesthetized rats in vivo, at 11 to 40 days

Accepted August 18, 2005.
Address correspondence and reprint requests to Dr. L. Stan Leung at Department of Physiology & Pharmacology, Medical Sciences Bldg, Rm 216, University of Western Ontario, London, Ontario, Canada N6A 5C2. E-mail: sleung@uwo.ca
Previously presented in part at the annual meeting of the American Epilepsy Society, December 3, 2004, New Orleans, Louisiana, U.S.A.

after hyperthermic seizures. Early (<100 ms) paired-pulse inhibition (PPI) of the population spikes is mediated by $GABA_A$ receptors (15–17), whereas the late (>100 ms) PPI is mediated by $GABA_B$ receptors (18, 19). Pharmacologic blockade of either $GABA_A$ (11) or $GABA_B$ receptor function (20,21) induced seizures. We are not aware of any study of excitatory or inhibitory synaptic transmission in vivo after hyperthermia-induced seizures.

MATERIALS AND METHODS

Subjects

Procedures were approved by the Animal Use Committee at the University of Western Ontario. Litters of Long-Evan immature rats, aged 10 days with the dam, were obtained from Charles River, Quebec, Canada. Pups were housed with their mother until weaning at postnatal day (PND) 21. Animals had free access to food and water ad libitum, and maintained on a 12-h light/12-h dark schedule.

Hyperthermia-induced seizures

Hyperthermic seizures were induced from rats of PND 13–15. The rat's brain at ~PND 14 was considered equivalent in development to a human brain of several months to 2–3 years of age (22,23). Two procedures were used to induce seizures: (a) a single hyperthermic seizure was given by a heat lamp on PND 15, and (b) repeated hyperthermic seizures were induced by heated air from a hair dryer on PND 13 to 15. Siblings of the seizure rats were used as controls, and they were placed in a chamber at room temperature. Duration of separation of a pup from its mother was similar in control and seizure rats. In another control group ("hyperthermia control" group), pups were injected with sodium pentobarbital (PTB; 30 mg/kg, i.p.) before heating with a heat lamp until the core temperature reached 41 to 43°C. No behavioral seizure was observed during hyperthermia in the "hyperthermia control" group.

In the lamp single-seizure treatment, an infrared heat lamp (660 watts) was held ~16 cm above the rat in a 20.5 × 20.5 × 22-cm plastic container, with the floor covered with non–heat-absorbing styrofoam. Immature rats reached a body temperature of 41 to 43°C in 5.8 ± 0.5 min when generalized convulsions were observed. The temperature of air within the container was checked every 30 s, and the body temperature of the rat was measured every 2 min by using an ear thermoprobe. The ear thermoprobe was adjusted to read the same as the rectal temperature. After the onset of a convulsive seizure, pups were cooled by placing them on a cold surface (a plastic bag containing ice) until they were responsive, and then transferring them under room temperature until their core temperature returned to baseline. The pups were observed until they could walk voluntarily, and then they were returned to their home cage and rehydrated with saline injections.

In the heated-air repeated-seizure treatment, a hair dryer at moderate heat setting (500 watts) was used to blow hot air down from the top of a 3-L glass container, ~50 cm above a rat (24). The bottom of the container sat in a water bath maintained at 37°C, to prevent overheating (10). The ear temperature of the pups was measured before heating, at 2-min intervals during heating, and at the onset of a seizure. The behavior was monitored and recorded by a video camera. After ≥10 min of behavioral seizures or at a high core body temperature (40–43°C), the pups were placed on a cool surface until they recovered. The duration of heating for each session was 21.20 ± 1.29 min. Hyperthermic seizures were induced at an interval of 4 h, three per day, starting at PND 13, for 3 consecutive days and a total of nine seizures (10). No hyperthermia control group was included for repeated seizures, because this would involve prolonged sedation by pentobarbital for ≥12 hours each day for 3 days. Other studies indicated that hyperthermia per se did not result in neuronal injury or change in neuronal inhibition (9,12,25).

A separate group of pups at PND 13 (n = 8) were implanted for electrical seizure detection. Under PTB anesthesia (30–35 mg/kg, i.p.), holes were drilled in the skull for placing electrodes in the dorsal hippocampus at P (posterior to bregma) 3.0 mm, L (lateral from midline) 2.1 mm, V (ventral from the skull surface) 3.0 mm, basolateral amygdala (P 1.8, L 3.7, V 8.0), parietal cortex (P 3.0, L 2.1, V 1.3), frontal cortex (P 0.0, L 0.2, V 1.3), and visual cortex (P 5.0, L 2.8, V 1.3) (26). Each electrode was a Teflon-insulated wire of 125 μm soldered to a connector pin, and the pins were embedded in dental cement and secured to screws in the skull. Two days later, EEG was recorded on a polygraph (Grass 7D).

Electrophysiological recordings and data analysis

Hippocampal electrophysiology was studied at two time periods after hyperthermic or control treatment: 11–18 days (called 14 days for short) or 28–40 days (called 30 days). Rats were anesthetized with urethane (1.2 g/kg, i.p.), and atropine methyl nitrate (0.12–0.17 mg/kg, i.p.) was injected to prevent fluid accumulation in the airway. Rats were then placed in a stereotaxic frame with appropriate ear bars. Stimulation of CA3 stratum radiatum [P 2.8–3.2, L 3.0–3.2, V 3.0–3.2 by using Paxinos and Watson's atlas (27)] was used to orthodromically activate the apical dendritic synapses of CA1 through the Schaffer collaterals (28). Stimulation of the medial perforant path (MPP) at P 7–8, L 4.4, and V 2.8–3.2 mm orthodromically excited the DG (29).

Laminar profiles of evoked field potentials in the hippocampus were recorded simultaneously by a silicon probe (28), placed at P 3.2–3.8, L 2.2–2.6. The silicon probe, fabricated by the NIH Center for Communications Technology at the University of Michigan, consisted of 16 electrodes located 50 μm apart on a vertical shank. Thus

the probe recorded field potentials over a depth of 750 μm, and it was lowered to record from CA1 (V 2.7–3.2) and then the DG (V 3.6–4.0).

Paired-pulse responses at 50-ms and 200-ms interpulse intervals (IPIs) were recorded at various intensities (input–output or I/O profiles) ranging from threshold to maximum of the population spike. Paired pulses were repeated at >10-s intervals. With an intensity that evoked ~80% of the maximum of first-pulse population spike (PS), paired pulses of IPI of 30–400 ms in CA1 and 20–800 ms or 30–400 ms in the DG were recorded. Single sweeps and their average (typically of four sweeps) were stored by a custom program. The field potentials recorded at one time instant were subjected to current source density (CSD) analysis. The latter is the inverse process of deriving the current sources and sinks that generate a field potential (30,31). At the site of the excitatory synapses at the apical dendrites, excitatory postsynaptic potential (EPSP) currents are inward, and the CSD shows a current sink. The soma and distal dendrites provide passive outward currents (current source) that complete a current loop with the inward synaptic current (31). Similarly, at the site of spike firing near the cell body, the cell body layer shows an inward current and a sharp current sink, and the apical dendrites provide the current source. Assuming a mainly longitudinal, one-dimensional current flow, the CSD at a particular depth was approximated by the equation (31,32)

$$\mathrm{CSD}(z, t) = \sigma[2\Phi(z, t) - \Phi(z + \Delta z, t) - \Phi(z - \Delta z, t)]/(\Delta z)^2$$

where $\Phi(z, t)$ is the potential at depth z and time t, and Δz (50 μm) is the space between adjacent electrodes on the silicon probe. No smoothing of CSD and potential was necessary for silicon probe recordings. The conductivity σ was assumed to be constant, and the CSDs are reported in units of V/mm^2.

The field potential consisted of extracellular or population EPSP (pEPSP) and population spike (PS) components (29,32). Measures of the field EPSP and PS were determined from the CSDs. PS was measured by the amplitude of the fast sink at the CA1 cell layer—a tangent line was extrapolated to join the positive peaks that surround the spike sink (minimum), and the amplitude of the PS was the vertical distance from sink minimum to the tangent line. The slope of pEPSPs was measured at the site of the maximal pEPSP sink at stratum radiatum of CA1; the slope was measured on the rising pEPSP sink over duration of 1 ms, ≥0.5 ms before the onset of a PS. In the DG, the pEPSP slope and PS amplitude were analyzed at the middle molecular layer and granular cell layer, respectively. P1 and P2 were, respectively, the PS amplitudes after the first and the second pulse, whereas E1 and E2 were, respectively, the slopes of pEPSPs after the first and the second pulse. The ratio of evoked PSs (P2/P1) was used to estimate PPI and facilitation. P2/P1 <1 indicates PPI, and P2/P1 >1 indicates paired-pulse facilitation (PPF).

In some experiments, the effect of the specific $GABA_B$-receptor antagonist 3-amino-propyl-diethoxy-methyl-phosphinic acid (CGP35348; a gift from W. Froestl of Novartis), on PPI was studied. A 23-gauge tubing was placed over the lateral ventricle (P 0.8, L 1.4, V 4.6), and baseline recordings were made. At the time of injection, 93 μg (400 nmoles) of CGP35348 dissolved in 1.33 μl of saline was injected intracerebroventricularly (icv) by a 26-gauge cannula into the lateral ventricle. Assuming a ventricular cerebrospinal fluid (CSF) volume of 1.5 ml, the resulting concentration of CGP35348 in the CSF was estimated to be 266 μM. The latter dose was determined to be effective in blocking postsynaptic $GABA_B$receptor–mediated responses assessed by PPI in rats in vivo (21,33). In separate groups of rats of ~PND30, one fourth of the selected dose (100 nmoles CGP35348, icv) gave a smaller effect, whereas 800 nmoles, icv, gave a similar effect. An IPI profile at 80% maximal stimulus intensity and I/O curves at 50 ms and 200 ms IPIs were recorded before and after drug injection.

At the end of recording, the position of a stimulating electrode was marked by passing a direct current of 0.3 mA for 1 s, resulting in a lesion of ~0.5 mm radius. No lesion was made at the recording silicon probe, because the cell layer could be clearly indicated by electrophysiologic criteria (Results). Under deep anesthesia, the rat was perfused with 4% buffered formalin. Subsequently, the brain was cut into 40-μm-thick coronal sections by using a cryomicrotome and stained with thionin to verify the electrode placement.

Data are presented as mean ± SEM. Statistical significance was assessed by repeated-measures analysis of variance (ANOVA). A significant ANOVA was followed by post hoc Newman–Keuls test. Differences were considered significant if $p < 0.05$.

RESULTS

Experiment 1: Seizure behavior and EEGs during hyperthermic seizures

A hyperthermic seizure induced by a heat lamp in PND15 rat pups typically started with hindlimb kicks, followed by generalized tonic and clonic convulsions of four limbs while lying down, and ending with a long period of postictal immobility during which the pup was unresponsive to sensory stimuli (Table 1). Hippocampal EEGs showed a slight depression or a slow (~2 Hz) oscillation at the start of behavioral convulsions, but often broke into a high-amplitude afterdischarge after the generalized tonic–clonic convulsions (Fig. 1A). Occasionally, independent sharp waves (~1 Hz) were observed in the neocortical electrodes during the behavioral seizure. Repeated lamp

TABLE 1. *Number of seizures showing a type of behavior during hyperthermic seizure induced by a heat lamp or heated air in rat pups of postnatal days 13–15*

	Heat lamp	Heated air
Number of seizures	19 seizures	63 seizures
Hindlimb kicks	16 (84.2%)	17 (27.0%)
Mouth automatisms	4 (21%)	45 (71.4%)
Immobility associated with tonic flexion of body	17 (89.4%)	63 (100%)
Squeak	11 (64.7%)	4 (6.3%)
Tonic and clonic twitching of four limbs while lying down	12 (63.2%)	10 (15.9%)
Prolonged postictal immobility	15 (78.9%), not responsive	63 (100%), responsive
Myoclonic jerks	0	57 (90.5%)
Duration of seizure	5.8 ± 0.5 min	21.2 ± 1.3 min

induced seizures were precluded because of high fatality and severity of these seizures.

Seizures induced by heated air in PND13–15 rat pups typically showed oral automatisms, myoclonic jerks, immobility with tonic body flexion, and hindlimb kicking, with very few seizures showing clonic jerks while lying down (Table 1). Abnormal sharp events in the EEG (Fig. 1B) were seen in the amygdala and hippocampus during oral automatisms, immobility, and behavioral seizures. Independent sharp waves were also seen in the neocortex during the behavioral seizures (Fig. 1B). During the postictal immobility after a heated-air seizure, the pup was usually responsive to sensory stimuli. In both heat-lamp– and heated-air–induced seizures, the hippocampus appeared to be a major participant.

Experiment 2: Assessment of neuronal inhibition in the hippocampus at 14 days and 30 days after heat-lamp–induced single seizures

Stimulation of CA3 (Fig. 2, inset) evoked inward excitatory postsynaptic currents at the apical dendrites, shown as a current sink at stratum radiatum (SR, shaded gray in Fig. 2). The sink was accompanied by current sources at the CA1 cell layer or stratum pyramidale (SP in Fig. 2) and distal dendrites ($\geq$400 μm depth). The synchronous firing of the pyramidal cells resulted in a population spike, shown as a sharp negative sink at the cell layer (stripped area at SP in Fig. 2). Thresholds for the first-pulse pEPSP (E1) and population spike (P1) in CA1 were 74 ± 3 μA (n = 8) and 185 ± 31 μA (n = 8) in control rats and did not differ between control and seizure animals. The "hyperthermia control" rats given hyperthermia with

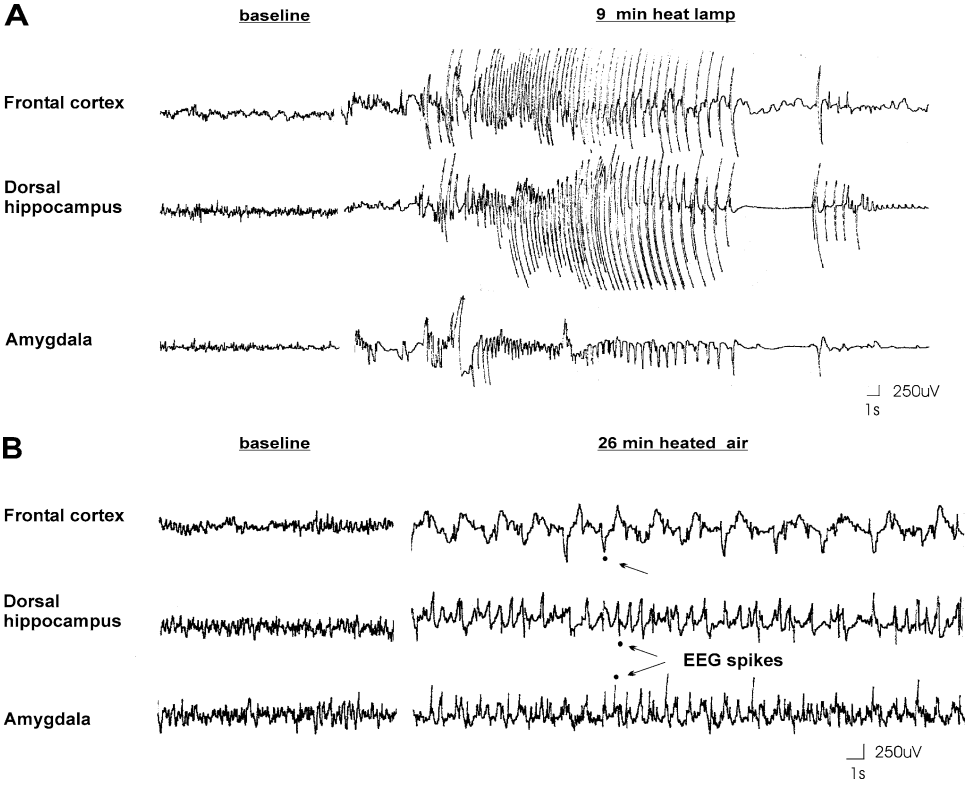

FIG. 1. Representative EEG traces in 15-day-old immature rats before and during heating by an **(A)** heat lamp or **(B)** hair dryer. **A:** Baseline recordings (*left*) show normal EEG before applying a heat lamp. At 9 min of heating by a heat lamp and a body temperature of 43.0°C, behavioral convulsions were observed with hindlimb kicks, squeaks, tonic extension, and clonic jerks of four limbs. At the end of the convulsion, an afterdischarge was observed at the hippocampus and frontal cortex, spread to the amygdala, and followed by postictal depression. **B:** At 26 min of heating by a hair dryer (ambient temperature 50°C and body temperature 42.5°C), EEG showed stereotyped spikes at the hippocampus and amygdala, and paroxysmal activity at the frontal cortex associated with immobility and head nodding.

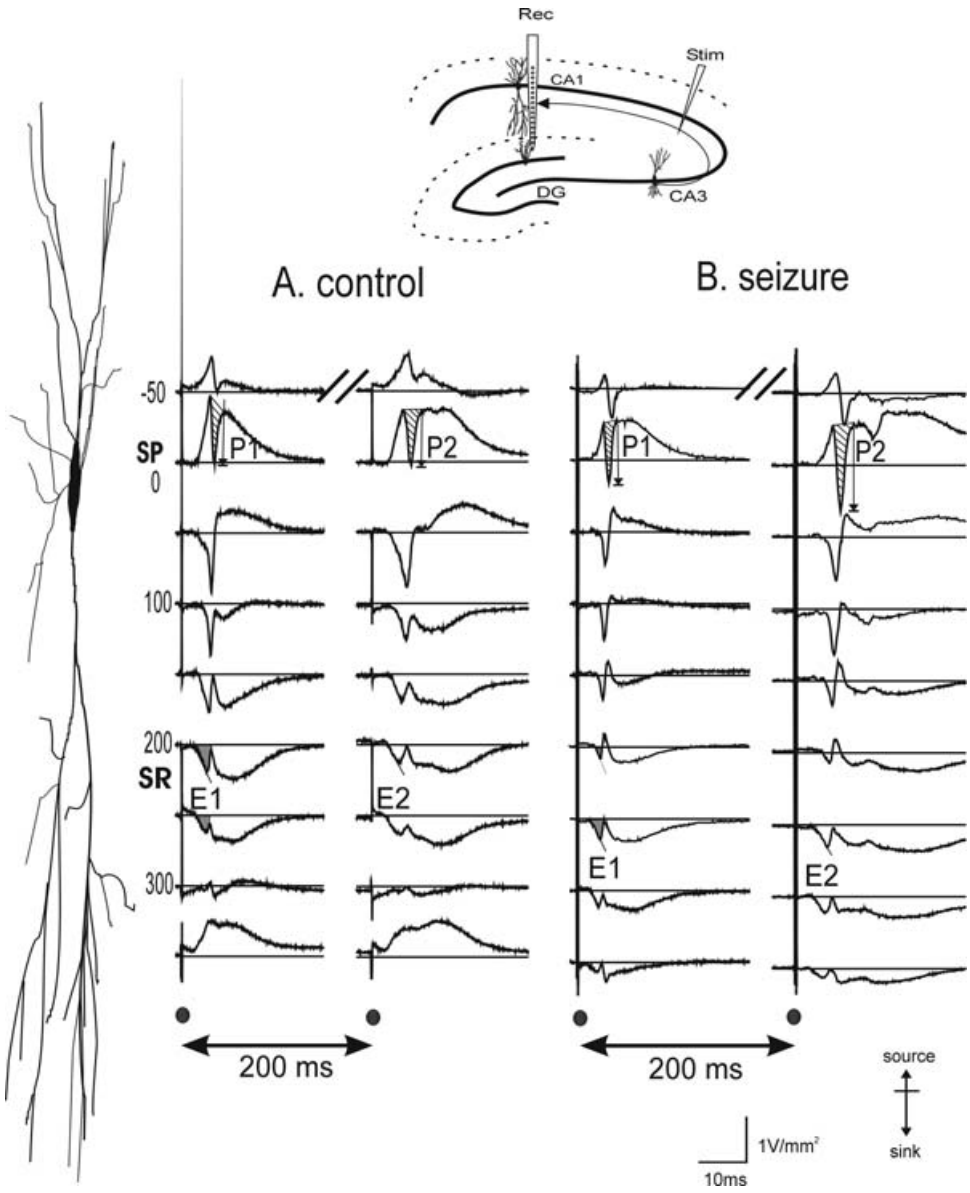

FIG. 2. Paired-pulse facilitation in CA1 was observed 14 days after a single hyperthermic seizure. **Top inset,** schematic of 16-channel recording (Rec) in CA1 and CA3 stimulation (Stim). Current source density (CSD) profiles (not all traces shown) after a pair of stimulation pulses of 200-ms interpulse interval are shown in a control rat **(A)** and a hyperthermic seizure rat **(B)** at 14 days after treatment. **Left side,** a CA1 pyramidal cell is illustrated with depth (μm) away from the CA1 pyramidal cell layer (SP), assumed to be at 0 μm, and increasing positive depth toward the apical dendrites. Population spikes (after the first and second stimulus pulses, P1 and P2, respectively) were measured at the CA1 cell layer, and slopes of excitatory postsynaptic potentials (after the first and second pulses, E1 and E2, respectively) were measured in striatum radiatum (SR). Note P2 $>$ P1 in the seizure rat but not the control rat. *Black solid circles* indicate stimulation artifacts. CSD was shown with source up.

pentobarbital (PTB) were not significantly different from the nonheated control rats in P2/P1 (Fig. 3A) or other measures analyzed.

Paired-pulse population spike responses were different between control and seizure rats. In control rats, paired-pulse stimulation at $<$150 ms IPIs resulted in suppression of the second-pulse population spikes (P2) as compared with first-pulse population spike (P1), or P2/P1 $<$1. P2/P1 $\approx$1 was found at 150- to 400-ms IPIs (Fig.3A). In contrast, in seizure rats recorded 14 days after a single heat-lamp seizure, PPF (P2/P1 $>$1) was found at $>$100-ms IPIs (Fig. 2B; Fig. 3A), significantly larger than P2/P1 in the control rats. Repeated-measures ANOVA gave a significant Group effect ($F_{1,13} = 5.04$; $p = 0.041$), and a trend of a Group $\times$ IPI interaction ($F_{4,48} = 2.46$; $p = 0.058$). Post hoc Newman–Keuls test revealed significant P2/P1 differences at 150- and 200-ms IPIs ($p < 0.05$). When recorded 30 days after a single seizure, no significant

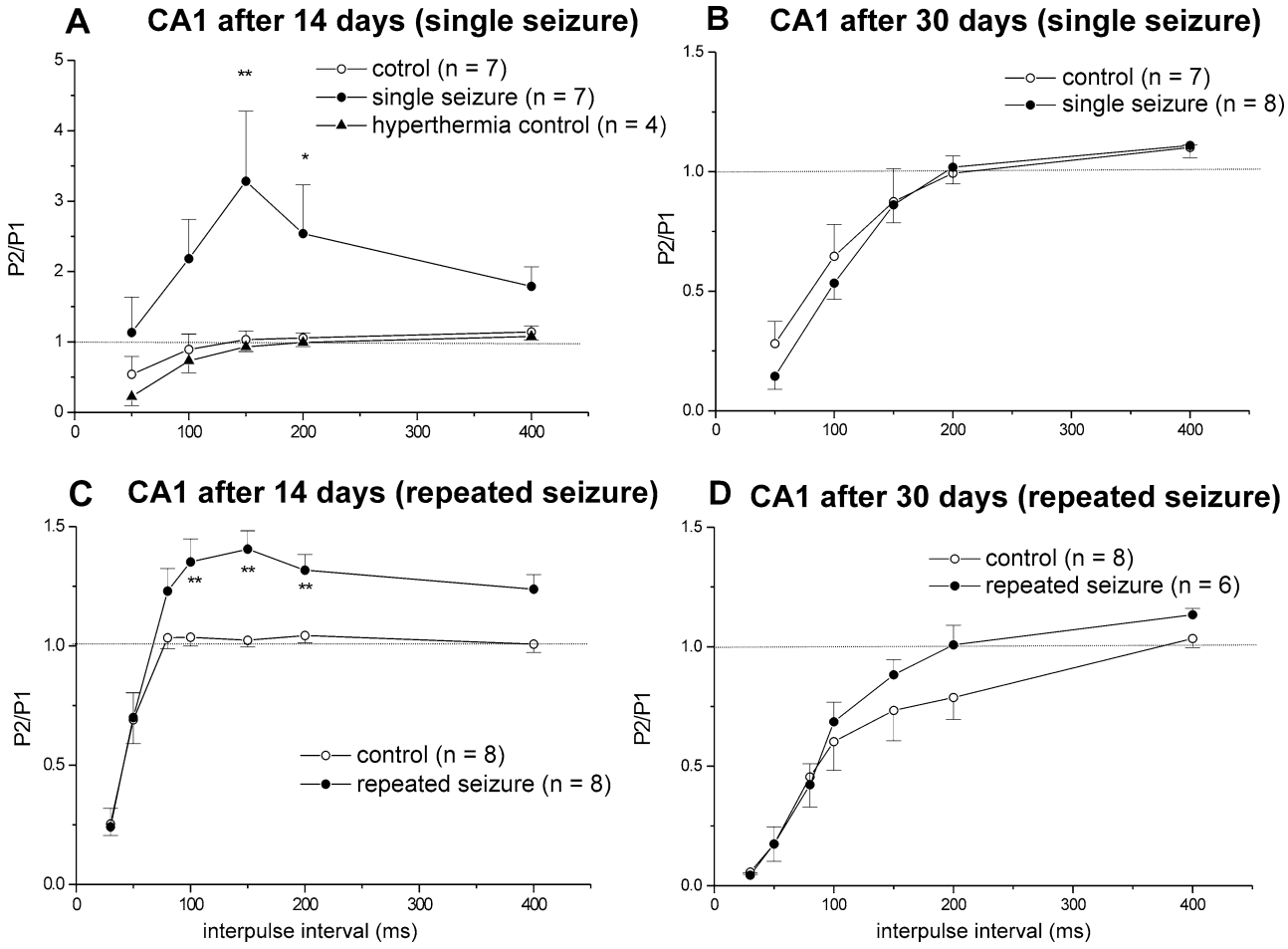

FIG. 3. Increased paired-pulse facilitation of population spikes (P2/P1) in CA1, shown as plots of P2/P1 (means ± standard error of the mean, SEM) versus interpulse interval, was found at 14 but not 30 days after hyperthermic seizure(s). **A:** P2/P1 ratio was significantly larger in the single-seizure group, as compared with the control group, 14 days after treatment. The hyperthermia control group that was heated after pentobarbital (see Methods) responded similar to the nonheated control group. **B:** No statistical difference in P2/P1 in CA1 was found between single-seizure and control rats at 30 days after treatment. **C:** P2/P1 ratio was significantly larger in the repeated-seizure group, as compared with controls. **D:** No difference was found in P2/P1 in CA1 between repeated-seizure and control rats at 30 days after treatment. In **A** and **C**, $*p < 0.05$, $**p < 0.01$, post hoc Newman–Keuls test after repeated-measures ANOVA.

difference was found between seizure and control rats in the P2/P1 versus IPI relation ($F_{1,14} = 0.26$; $p = 0.62$; Fig. 3B). Both seizure and control rats showed PPI (P2/P1 <1) in CA1 at <150 ms IPI, and small PPF at IPI > 200 ms (Fig. 3B).

Stimulation of MPP resulted in a pEPSP sink at the middle molecular layer of the DG. At the granule cell layer, pEPSP is shown as a source that was followed by the population spike sink (Fig. 4A, inset). The stimulus thresholds for the pEPSP and P1 in the DG were 48 ± 7 μA (n = 7) and 177 ± 46 μA (n = 7) in control rats, respectively, not significantly different from corresponding values in seizure rats. After a single hyperthermic seizure, P2/P1 as a function of IPI was not different between seizure and control rats in the DG, at 14 days (Fig. 4A; $F_{1,13} = 0.46$, $p = 0.51$) or 30 days after treatment (Fig. 4B; $F_{1,13} = 0.33$, $p = 0.58$).

Experiment 3: Assessment of neuronal inhibition in CA1 and DG at 14 and 30 days after heated-air–induced repeated seizures

Similar to results after a single seizure, repeated heated-air seizures resulted in an increase of P2/P1 in CA1 compared with controls at 14 days but not 30 days after seizure treatment. At 14 days after treatment, P2/P1 in CA1 was different in repeated-seizure rats as compared with controls (Fig. 3C), as shown by repeated-measures ANOVA, giving a significant Group effect ($F_{1,15} = 10.62$; $p = 0.0057$) and a significant Group × IPI interaction ($F_{6,84} = 3.57$; $p = 0.0034$). The P2/P1 differences at 100-, 150-, and 200-ms IPIs shown in Fig. 3C were significant by post hoc Newman–Keuls tests. A scatterplot of P2 versus P1 (not shown) showed that the larger P2/P1 ratio in the seizure rats was independent of changes in P1. When CA1 was recorded 30 days after treatment, P2/P1 was

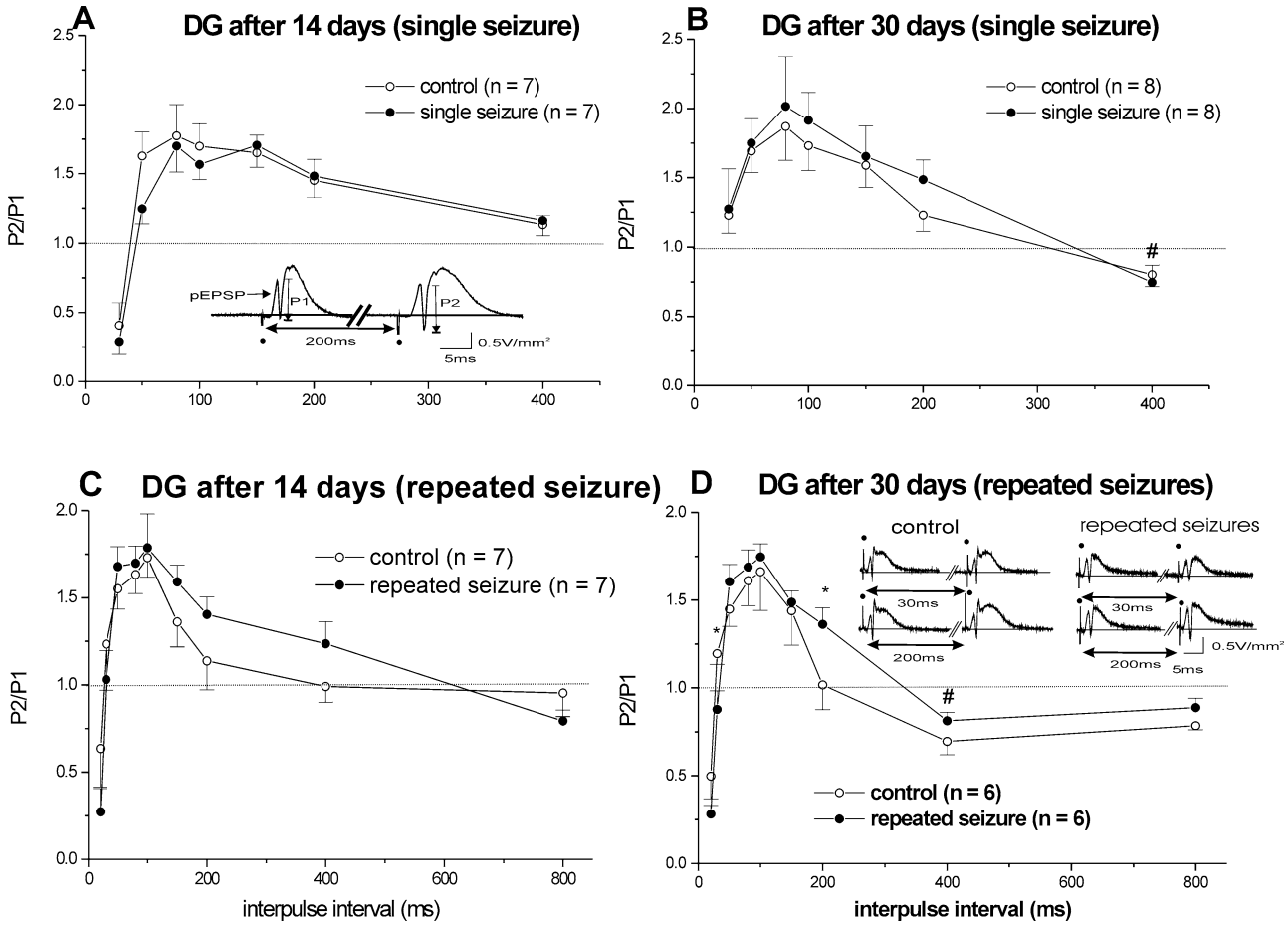

FIG. 4. Plots of the paired-pulse ratio of population spikes (P2/P1) versus interpulse interval in the dentate gyrus (after medial perforant-path stimulation). **Inset in A** is an example of the current source density (CSD) derived from the DG granular cell layer, with population excitatory postsynaptic potential (pEPSP) measured as a slope and population spike after the first (P1) and second pulse (P2) measured as amplitudes. P2/P1 values (mean ± SEM) are not different between seizure and control rats at **(A)** 14 days and **(B)** 30 days after a single hyperthermic seizure or at **(C)** 14 days after repeated hyperthermic seizures. **D:** P2/P1 ratio was significant decreased at 30-ms and increased at 200-ms interpulse intervals. **Inset in D** shows CSD profiles in the DG granular cell layer between control and seizure rats after 30 days of treatment. Paired-pulse inhibition at 400-ms interpulse interval (P2/P1 < 1, # in **B** and **D**) was found in both control and seizure rats in older (∼45 days old, **B** and **D**) but not younger (∼30 days old, **A** and **C**) rats. In **D**, $*p < 0.05$, post hoc Newman–Keuls test after repeated-measures ANOVA. *Black solid circles* indicate stimulation artifacts.

larger in repeated-seizure rats as compared with controls (Fig. 3D), but the difference was not statistically significant, as shown by repeated-measures ANOVA ($F_{1,11} = 0.68$, $p = 0.43$ for Group effect; $F_{6,60} = 1.34$, $p = 0.25$ for Group × IPI interaction). The P2/P1 ratio in CA1 was smaller for 30- to 200-ms IPIs in the older rats (Fig. 3D) as compared with immature rats (Fig. 3C). The latter suggests an increase in inhibition with maturation, consistent with previous studies (34).

Differences in the DG were found at 30 days but not 14 days after repeated seizures in rats compared with control rats. At 14 days after treatment, no significant difference was found between repeated-seizure and control rats in the P2/P1 versus IPI relation in the DG (Fig. 4C), as confirmed by repeated-measures ANOVA ($F_{1,13} = 0.48$; $p = 0.50$ for Group effect; $F_{8,96} = 0.43$, $p = 0.90$ for Group × IPI interaction). At 30 days after treatment, the P2/P1 versus IPI relation was different between repeated-seizure and control rats (Fig. 4D), as shown by a significant Group × IPI interaction ($F_{6,60} = 2.68$; $p = 0.02$) without a Group effect ($F_{1,11} = 0.21$; $p = 0.66$) after repeated-measures ANOVA. Post hoc Neuman–Keuls tests showed a P2/P1 decrease at 30-ms IPI and a P2/P1 increase at 200 ms in repeated-seizure rats as compared with controls (Fig. 4D).

Long-latency PPI in the DG increased in the older as compared with immature rats. PPI at 400-ms IPI was only found in older rats (recorded on ∼PND 44; # in Fig. 4B and D) as compared with younger ones (recorded on ∼PND 29; Fig. 4A and C). Maturation of the PPI at ∼400-ms IPI in the DG was previously reported by using comparison between PND16 and adult (PND60) rats (34) or between PND30 and adult rats (35).

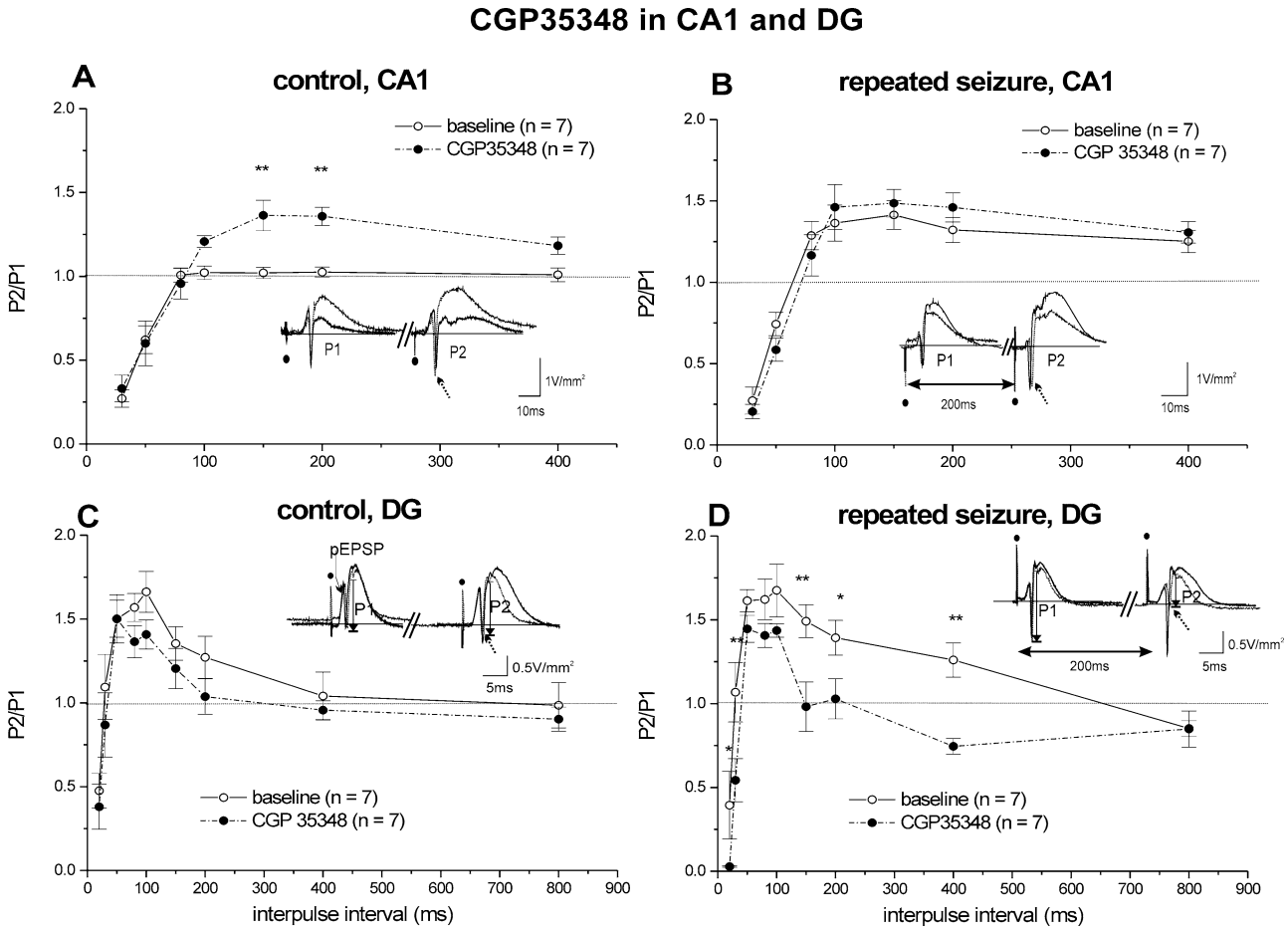

FIG. 5. Intracerebroventricular (icv) injection of $GABA_B$-receptor antagonist CGP35348 increased paired-pulse facilitation of the population spikes in CA1 in control but not in repeated-seizure rats at 14 days after treatment. In the dentate gyrus (DG), icv CGP35348 increased paired-pulse inhibition in repeated-seizure rats. **A:** Paired-pulse population spike ratio P2/P1 (mean ± SEM) versus interpulse interval (IPI) plots before and after icv CGP35348 injection in control rats. P2/P1 was significantly increased after CGP35348 injection, as compared with baseline before injection. **Inset** shows an increase in P2 but not P1 after CGP35348 (*dotted trace*) compared with baseline (*solid trace*) in an example of the current source density (CSD) from the CA1 pyramidal cell layer. **B:** Same plots as **A** except for rats after repeated seizures. CGP35348 (icv) did not significantly alter P2/P1 ratio at different IPIs. **Inset** shows a CSD trace for an individual repeated-seizure rat. **C:** In the DG of control rats, CGP35348 icv injection did not significantly decrease the P2/P1 ratio, as compared with baseline. CSD example **(inset)** shows little change in P2 after CGP 35348 (*dotted trace*) compared with baseline (*solid trace*) from the DG granule cell layer. P2 amplitude after CGP35348 was illustrated by the *vertical down arrow* above the *slanted dotted arrow*. **D:** In seizure rats, CGP35348 significantly decreased P2/P1 ratio as compared with baseline. *Inset CSD trace* shows CGP35348 decreased P2 more in a seizure rat. In **A** and **D**, $*p < 0.05$, $**p < 0.01$, post hoc Newman–Keuls test.

Experiment 4: Effects of $GABA_B$-antagonist CGP35348 on PPI in the hippocampus at 14 days after heated-air–induced repeated seizures

We hypothesize that the increase in P2/P1 ratio at 100- to 400-ms IPI in CA1 of seizure rats was caused by a decrease in a late inhibition mediated by postsynaptic $GABA_B$ receptors. To verify this hypothesis, we injected specific $GABA_B$-receptor antagonist CGP35348, icv, in control and seizure rats, 14 days after repeated seizures or control treatment.

Injection of icv CGP35348 did not significantly change the threshold or amplitude of the first-pulse response (P1 or E1), in either seizure or control group (data not shown). However, icv CGP35348 increased the P2/P1 ratio at 100- to 400-ms IPI in control rats (Fig. 5A). The drug effect (comparing before and after CGP35348) was significant ($F_{1,6} = 7.16$; $p = 0.03$), and the Drug × IPI interaction also was significant ($F_{6,36} = 6.13$; $p = 0.0002$). Post hoc Newman–Keuls tests revealed statistical significance at 150- and 200-ms IPIs (Fig. 5A). In contrast, after icv CGP35348 injection in repeated-seizure rats, the P2/P1 ratio in CA1 was not significantly changed (Fig. 5B). Repeated-measures ANOVA showed no significant drug effect ($F_{1,6} = 0.0047$; $p = 0.95$) or Drug × IPI interaction ($F_{6,36} = 1.86$; $p = 0.10$).

In the DG, icv CGP35348 injection tended to suppress the P2 amplitude at 100- to 400-ms IPI without changing P1 amplitude (Fig. 5C). The decrease in P2/P1 ratio after icv CGP35348 injection in the control rats was small and did not reach statistical significance (Drug effect, $F_{1,6} =$

5.06; $p = 0.07$; Interaction effect, $F_{8,48} = 0.41$; $p = 0.91$; Fig. 5C). In repeated-seizure rats, icv CGP35348 injection significantly decreased P2/P1 ratio (Fig. 5D). Repeated-measures ANOVA yielded a significant Drug effect ($F_{1,6} = 57.85$; $p = 0.0003$) and a significant Drug × IPI interaction ($F_{8,48} = 2.52$; $p = 0.02$). Post hoc Newman–Keuls tests revealed significant differences in P2/P1 at 20-, 30-, 150-, 200-, and 400-ms IPIs (Fig. 5D). CGP35348, icv, did not significantly change P1 or E1 measures in the DG.

Thirty days after repeated seizures, the effect of icv CGP35348 in the DG was similar to that at 14 days after seizures. P2/P1 was decreased after icv CGP35348 injection with a significant Drug effect ($F_{1,5} = 15.54$; $p = 0.01$) and a significant Drug × IPI interaction ($F_{8,40} = 3.09$; $p = 0.0083$). Post hoc Newman–Keuls test showed a significant decrease of P2/P1 at 30-, 150-, and 200-ms IPIs ($p < 0.01$). In contrast, control rats given icv CGP35348 did not show a significant drug effect on P2/P1 ($F_{1,4} = 2.24$; $p = 0.21$) or Drug × IPI interaction ($F_{8,32} = 1.84$; $p = 0.11$).

DISCUSSION

An increase in late PPF in CA1 was found at 14 days but not at 30 days after heat-lamp–induced single or heated-air-induced repeated hyperthermic seizures. We infer that the increase in late PPF was caused by a loss of $GABA_B$ receptor–mediated inhibition, because $GABA_B$-receptor blockade by icv CGP35348 increased PPF in CA1 of control rats. In addition, CGP35348 did not significantly change PPF in CA1 of seizure rats, suggesting that no postsynaptic $GABA_B$ receptors were present to block. A similar decrease of postsynaptic $GABA_B$ receptors was also suggested for the DG at 14 and 30 days after repeated heated-air induced seizures, as discussed later.

Behaviors and EEG during hyperthermia-induced seizures

Behavioral and EEG characteristics were somewhat different for the two hyperthermic-seizure models used, but the hippocampus showed paroxysmal activity in both models. In the heated-air procedure, abnormal EEGs were observed first in the amygdala and dorsal hippocampus before the neocortex. This is consistent with the amygdala as an early site for hyperthermic seizures induced by heated air (24), and mouth automatisms were observed during seizures kindled from the amygdala (36). In the heat-lamp procedure, high-amplitude hippocampal afterdischarges usually followed generalized convulsions. The severity and high mortality of heat-lamp seizures, which may involve brainstem-induced tonic limb extension (37), preclude the use of repeated heat-lamp seizures.

Inducing hyperthermia in immature animals is the most commonly used animal model to study febrile seizures (8–10,24). Our results supported the findings of Baram et al. (24) that heated-air–induced seizures in immature rats give an appropriate-aged model suitable for long-term studies. The severity of a single heat-lamp seizure made it difficult to use for repeated seizures and perhaps less appropriate as a FS model. However, both heat-lamp and heated air seizures involved the hippocampus, although at different stages, and both resulted in alteration of synaptic transmission in the hippocampus.

Loss of $GABA_B$ receptor–mediated paired-pulse inhibition in CA1

Facilitation of paired-pulse response at long latencies (100- to 200-ms IPIs) was demonstrated at 14 days after seizure(s), irrespective of whether a single heat-lamp seizure or repeated heated-air seizures were evoked. We showed that icv injection of a specific $GABA_B$-receptor antagonist increased PPF (or decreased PPI) at 100 to 200 ms in control adult rats (Fig. 5A), confirming previous results (18). The increase in P2/P1 at 100- to 200-ms IPI is explained by blocking late postsynaptic $GABA_B$-receptor–mediated inhibition in CA1 neurons (11, 38–40). Rats after a single or repeated hyperthermic seizures showed increased PPF at 100 to 200 ms in CA1, similar to control rats after $GABA_B$-receptor blockade by icv CGP35348 (Fig. 5). Thus postsynaptic $GABA_B$-mediated inhibition in CA1 was inferred to be smaller in seizure rats, as compared with control rats.

Injection of $GABA_B$-receptor antagonist CGP35348 (icv) abolished the difference in PPI between seizure and control animals. In the seizure rat, the $GABA_B$-receptor antagonist CGP35348 did not change P2/P1, suggesting that $GABA_B$ postsynaptic inhibition was already lost, and thus pharmacologic blockade of $GABA_B$ receptors would have no additional effect.

To our knowledge, this is the first time that inhibition, in particular $GABA_B$ receptor–mediated inhibition, was assessed in vivo after hyperthermic seizures. Hyperthermic seizures in immature rats were shown to increase $GABA_A$ receptor–mediated inhibition in hippocampal CA1 neurons in vitro (12). However, we found no significant change in the early paired-pulse response (<100 ms IPI) that presumably measured $GABA_A$ receptor–mediated inhibition in CA1 in vivo. Differences in inhibition in vitro and in vivo (41) may account for the different results. In other seizure models, a decrease in postsynaptic $GABA_B$ receptor–mediated inhibition in CA1 was shown after a model of status epilepticus (19,42) but not after partial hippocampal kindling (43). Kindling, however, was shown to decrease the efficacy of presynaptic $GABA_B$ autoreceptors (44).

Changes in neuronal inhibition after heated-air repeated seizures in the DG

At 30 days after repeated seizures, PPI in the DG was significantly increased at 30-ms IPI. Increased $GABA_A$ receptor–mediated inhibition in the DG has been reported

after various seizure models, including hippocampal kindling (15,45) and models of status epilepticus (28,46–48).

We suggest that the postsynaptic $GABA_B$receptor–mediated inhibition of DG granule cells decreased after repeated hyperthermic seizures. Significant increase in PPF in the DG at long IPIs was found at 30 days but not 14 days after repeated seizures. No significant change of late PPF in the DG was found at 14 or 30 days after a single heat-lamp seizure.

We interpret an increase in late PPF in DG, similar to that in CA1, as resulting from decreased postsynaptic $GABA_B$ receptors on principal cells (DG cells). Afterhyperpolarization and other factors have been suggested as the cause of the late PPI in the DG (49), but blockade of PPI by local hippocampal injection of $GABA_B$-receptor antagonist CGP35348 (50) is consistent with the present interpretation. However, icv CGP35348 injection did not significantly change late PPI in the DG of control rats because icv CGP35348 may normally have opposing effects on the late P2/P1 ratio. CGP35348's action on GABAergic interneurons in the DG decreases P2/P1, whereas its action directly on postsynaptic $GABA_B$ receptors on granule cells increases P2/P1. In hippocampal slices in vitro, CGP35348 increased both early and late PPI evoked by the perforant path (17,46), consistent with CGP35348's proposed action on increasing the evoked firing of GABAergic interneurons. In repeated-seizure rats, we suggest that the postsynaptic $GABA_B$ receptor–mediated inhibition on granule cells is decreased. Thus the predominant effect of CGP35348 in repeated-seizure rats was to increase GABAergic interneuronal firing and decrease P2/P1 at both early and late latencies (Fig. 5D). The decrease in late P2/P1 in the DG after icv CGP35348 was found 14 days after repeated seizures, even though no late P2/P1 increase was seen in the seizure compared with control rats at this time.

After status epilepticus induced by kainic acid, CGP35348 had no effect on the late inhibition in the DG in vitro, whereas CGP35348 increased late inhibition in control rats (20,46). In contrast, we report here that CGP35348 increased late DG inhibition in vivo in seizure as compared with control rats.

CONCLUSION

Loss of postsynaptic $GABA_B$-receptor function in the brain increases epileptogenesis (21) and enhances excitability induced by glutamate receptor (51) and voltage-dependent Ca^{2+} channels (52). At 2 weeks but not at 4 weeks after hyperthermic seizures in immature rats, injured neurons were reported in CA1 and CA3 (25), matching the duration and location of the pathophysiology reported here. However, we also showed that late PPI in the DG decreased at 30 days after repeated hyperthermic seizures, suggesting that inhibitory gating in the DG (53,54) may be compromised for a long duration after seizures. Disruption of hippocampal $GABA_B$-receptor inhibition may contribute to the cognitive deficits in adult rats (10).

It is not known that FSs in children would result in a loss of $GABA_B$ receptor–mediated inhibition in the hippocampus. Also, whether a loss of $GABA_B$ receptor–mediated inhibition plays a part in the development of adult-onset seizures after FSs in children requires further studies.

Acknowledgment: This work was supported by an operating grant from Canadian Institutes of Health Research (MOP-64433), the London Health Sciences Centre Internal Research Funds, and a Savoy Foundation studentship to M.L. Tsai. We thank Dr. Richard S. McLachlan for helpful discussion on the research project, and Pascal Peloquin and Dr. Bixia Shen for assistance.

REFERENCES

1. Rocca WA, Sharbrough FW, Hauser WA, et al. Risk factors for complex partial seizures: a population-based case-control study. *Ann Neurol* 1987;21:22–31.
2. VanLandingham KE, Heinz ER, Cavazos JE, et al. Magnetic resonance imaging evidence of hippocampal injury after prolonged focal febrile convulsions. *Ann Neurol* 1998;43:413–426.
3. Scott RC, King MD, Gadian DG, et al. Hippocampal abnormalities after prolonged febrile convulsions: a longitudinal MRI study. *Brain* 2003;126:2551–2557.
4. Dube C, Yu H, Nalcioglu O, et al. Serial MRI after experimental febrile seizures: altered T2 signal without neuronal death. *Ann Neurol* 2004;56:709–714.
5. Liebregts MT, McLachlan RS, Leung LS. Hyperthermia induces age-dependent changes in rat hippocampal excitability. *Ann Neurol* 2002;52:318–326.
6. Tancredi V, D'Arcangelo G, Zona C, et al. Induction of epileptiform activity by temperature elevation in hippocampal slices from young rats: an in vitro model for febrile seizures? *Epilepsia* 1992;33:228–234.
7. Wu J, Fisher RS. Hyperthermic spreading depressions in the immature rat hippocampal slice. *J Neurophysiol* 2000;84:1355–1360.
8. McCaughran JA Jr, Schechter N. Experimental febrile convulsions: long-term effects of hyperthermia-induced convulsions in the developing rat. *Epilepsia* 1982;23:173–183.
9. Dube C, Chen K, Eghbal-Ahmadi M, et al. Prolonged febrile seizures in the immature rat model enhance hippocampal excitability long term. *Ann Neurol* 2000;47:336–344.
10. Chang YC, Huang AM, Kuo YM, et al. Febrile seizures impair memory and cAMP response-element binding protein activation. *Ann Neurol* 2003;54:706–718.
11. Olsen RW, Avoli M. GABA and epileptogenesis. *Epilepsia* 1997;38:399–407.
12. Chen K, Baram TZ, Soltesz I. Febrile seizures in the developing brain result in persistent modification of neuronal excitability in limbic circuits. *Nat Med* 1999;5:888–894.
13. Chen K, Aradi I, Thon N, et al. Persistent modified h-channels after complex febrile seizures convert the seizure-induced enhancement of inhibition to hyperexcitability. *Nat Med* 2001;7:331–337.
14. Holmes GL, Ben-Ari Y. Seizures in the developing brain: perhaps not so benign after all. *Neuron* 1998;21:1231–1234.
15. Tuff LP, Racine RJ, Adamec R. The effects of kindling on GABA-mediated inhibition in the dentate gyrus of the rat, I: paired-pulse depression. *Brain Res* 1983;277:79–90.
16. Steffensen SC, Henriksen SJ. Effects of baclofen and bicuculline on inhibition in the fascia dentata and hippocampus regio superior. *Brain Res* 1991;538:46–53.

17. Haas KZ, Sperber EF, Moshe SL, et al. Kainic acid-induced seizures enhance dentate gyrus inhibition by downregulation of $GABA_B$ receptors. *J Neurosci* 1996;16:4250–4260.
18. Olpe HR, Steinmann MW, Ferrat T, et al. The actions of orally active $GABA_B$ receptor antagonists on GABAergic transmission in vivo and in vitro. *Eur J Pharmacol* 1993;233:179–186.
19. Wasterlain CG, Shirasaka Y, Mazarati AM, et al. Chronic epilepsy with damage restricted to the hippocampus: possible mechanisms. *Epilepsy Res* 1996;26:255–265.
20. Vergnes M, Boehrer A, Simler S, et al. Opposite effects of $GABA_B$ receptor antagonists on absences and convulsive seizures. *Eur J Pharmacol* 1997;332:245–255.
21. Leung LS, Canning KJ, Shen B. Hippocampal afterdischarges after $GABA_B$-receptor blockade in the freely moving rat. *Epilepsia* 2005;46:203–216.
22. Dobbing J, Sands J. Quantitative growth and development of human brain. *Arch Dis Child* 1973:48:757–767.
23. Avishai-Eliner S, Brunson KL, Sanderman CA, et al. Stressed-out, or in (utero)? *Trends Neurosci* 2002;25:518–524.
24. Baram TZ, Gerth A, Schultz L. Febrile seizures: an appropriate-aged model suitable for long-term studies. *Dev Brain Res* 1997;98:265–270.
25. Toth Z, Yan XX, Haftoglou S, et al. Seizure-induced neuronal injury: vulnerability to febrile seizures in an immature rat model. *J Neurosci* 1998;18:4285–4294.
26. Sherwood NM, Timiras PS. *A Stereotaxic Atlas of the Developing Rat Brain*. Berkeley: University of California Press, 1970.
27. Paxinos G, Watson C. *The Rat Brain in Stereotaxic Coordinates*, 2nd ed. San Diego: Academic Press, 1986.
28. Kloosterman F, Peloquin P, Leung LS. Apical and basal orthodromic population spikes in hippocampal CA1 in vivo show different origins and patterns of propagation. *J Neurophysiol* 2001;86:2435–2444.
29. Wu K, Leung LS. Enhanced but fragile inhibition in the dentate gyrus in vivo in the kainic acid model of temporal lobe epilepsy: a study using current source density analysis. *Neuroscience* 2001;104:379–396.
30. Freeman JA, Nicholson C. Experimental optimization of current source-density technique for anuran cerebellum. *J Neurophysiol* 1975;38:369–382.
31. Leung LS. Field potentials in the central nervous system: recording, analysis and modeling: neurophysiological techniques: applications to neural systems. In: Boulton AA, Baker GB, Vanderwolf CH, eds. *Neuromethods*. Clifton, NJ: Humana Press, 1990:277–312.
32. Anderson P, Bliss TV, Skreded KK. Lamellar organization of hippocampal pathway. *Exp Brain Res* 1971;13:222–238.
33. Karlsson G, Kolb C, Hausdorf A, et al. $GABA_B$ receptors in various in vitro and in vivo models of epilepsy: a study with $GABA_B$ receptor blocker CGP35348. *Neuroscience* 1992;47:63–68.
34. Bekenstein JW, Lothman EW. A comparison of the ontogeny of excitatory and inhibitory neurotransmission in the CA1 region and dentate gyrus of the rat hippocampal formation. *Dev Brain Res* 1991;63:237–243.
35. Bronzino JD, Blaise JH, Austin-LaFrance RJ, et al. Studies of dentate granule cell modulation: paired-pulse responses in freely moving rats at three ages. *Dev Brain Res* 1996;96:277–280.
36. Racine R. Modification of seizure activity by electrical stimulation, I: afterdischarge threshold, II: motor seizure. *Electroencephalogr Clin Neurophysiol* 1972;32:281–294.
37. Browning R, Maggio R, Sahibzada N, et al. Role of brainstem structures in seizures initiated from the deep prepiriform cortex of rats. *Epilepsia* 1993;34:393–407.
38. Lacaille JC. Postsynaptic potentials mediated by excitatory and inhibitory amino acids in interneurons of stratum pyramidale of the CA1 region of rat hippocampal slices in vitro. *J Neurophysiol* 1991;66:1441–1454.
39. Solis JM, Nicoll RA. Pharmacological characterization of $GABA_B$-mediated responses in the CA1 region of the rat hippocampal slice. *J Neurosci* 1992;12:3466–3472.
40. Davis CH, Starkey SJ, Pozza MF, et al. GABA autoreceptors regulate the induction of LTP. *Nature* 1991;349:609–611.
41. Buckmaster PS, Schwartzkroin PA. Interneurons and inhibition in the dentate gyrus of the rat in vivo. *J Neurosci* 1995;15:774–789.
42. Mangan PS, Lothman EW. Profound disturbances of pre- and postsynaptic $GABA_B$-receptor-mediated processes in region CA1 in a chronic model of temporal lobe epilepsy. *J Neurophysiol* 1996;76:1282–1296.
43. Liu X, Leung LS. Partial hippocampal kindling increase $GABA_B$ receptor-mediated postsynaptic currents in CA1 pyramidal cells. *Epilepsy Res* 2003;57:33–47.
44. Wu C, Leung LS. Partial hippocampal kindling decreases efficacy of presynaptic $GABA_B$ autoreceptors in CA1. *J Neurosci* 1997;17:9261–9269.
45. Leung LS, Zhao D, Shen B. Long-lasting effects of partial hippocampal kindling on hippocampal physiology and function. *Hippocampus* 1994;4:696–704.
46. Velisek L, Veliskova J. Estrogen treatment protects GABA(B) inhibition in the dentate gyrus of female rats after kainic acid-induced status epilepticus. *Epilepsia* 2002;43:146–151.
47. Gorter JA, van Vliet EA, Aronica E, et al. Long-lasting increased excitability differs in dentate gyrus vs. CA1 in freely moving chronic epileptic rats after electrically induced status epilepticus. *Hippocampus* 2002;12:311–324.
48. Wu K, Leung LS. Increased dendritic excitability in hippocampal CA1 in vivo in the kainic acid model of temporal lobe epilepsy: a study using current source density analysis. *Neuroscience* 2003;116:599–616.
49. Olpe HR, Karlsson G, Pozza MF, et al. CGP 35348: a centrally active blocker of $GABA_B$ receptor. *Eur J Pharmacol* 1990;187:27–38.
50. Canning KJ, Leung LS. Excitability of rat dentate gyrus granule cells in vivo is controlled by tonic and evoked $GABA_B$ receptor-mediated inhibition. *Brain Res* 2000;863:271–275.
51. Babcock AM, Everingham A, Paden CM, et al. Baclofen is neuroprotective and prevents loss of calcium/calmodulin-dependent protein kinase II immunoreactivity in the ischemic gerbil hippocampus. *J Neurosci Res* 2002;67:804–811.
52. Bertrand S, Nouel D, Morin F, et al. Gabapentin actions on Kir3 currents and N-type Ca^{2+} channels via $GABA_B$ receptors in hippocampal pyramidal cells. *Synapse* 2003;50:95–109.
53. Lothman EW, Stringer EH, Bertram EH. The dentate gyrus as a control point for seizures in the hippocampus and beyond. *Epilepsy Res Suppl* 1992;7:301–313.
54. Heinemann U, Beck H, Dreier JP, et al. The dentate gyrus as a regulated gate for propagation of epileptiform activity. *Epilepsy Res Suppl* 1992;7:273–280.